

Designed formation of $\text{Co}_3\text{O}_4@\text{NiCo}_2\text{O}_4$ sheets-in-cage nanostructure as high-performance anode material for lithium-ion batteries

Xuefeng Chu*, Chao Wang, Lu Zhou, Xingzhen Yan, Yaodan Chi and Xiaotian Yang *

Address: Jilin Provincial Key Laboratory of Architectural Electricity & Comprehensive Energy Saving, School of Electrical and Electronic Information Engineering, Jilin Jianzhu University, Changchun 130118, China.

E-mail: stone2009@126.com; hanyxt@163.com

Synthesis of ZIF-67 nanocrystals: Typically, 0.292 g of $\text{Co}(\text{NO}_3)_2 \cdot 6\text{H}_2\text{O}$ is dissolved in 25 mL of methanol, and 0.328 g of 2-methylimidazole is dissolved in another 25 mL of methanol. The two solutions are quickly mixed together, followed by aging for 24 hours at room temperature. Finally, the products are collected by centrifugation and dried at 60 °C overnight.

Synthesis of ZIF-67@NiCo-LDH yolk@shell nanoparticles: In a typical synthesis, 40 mg of ZIF-67 is dispersed in 25 mL of ethanol using ultrasound for five minutes. Then, 90 mg of $\text{Ni}(\text{NO}_3)_2 \cdot 6\text{H}_2\text{O}$ is added. 40 min later, the product is purified by centrifugation, washing with ethanol for three times and finally dispersed in 30 mL water for further use.

Synthesis of NiCo-LDH single-shelled nanoboxes: The synthesis is similar with the above mentioned the method for ZIF-67@NiCo-LDH yolk@shell nanoparticles. The only difference is further increasing the reaction time to three hours.

Synthesis of $\text{Co}(\text{OH})_2$ @NiCo-LDH sheets-in-cage nanoparticles: In a typical synthesis, 200 mg of HMT is dissolved in 10 mL of water. The as-obtained aqueous solution is added into the above ZIF-67@NiCo-LDH ethanol solution. Then, the mixture is heated in 90 °C in an oil bath for two hours. After cooling down to room temperature, the product is purified by centrifugation and washing with ethanol for three times.

Synthesis of Co_3O_4 @NiCo-LDH sheets-in-cage nanoparticles/ NiCo_2O_4 and Co_3O_4 nanocages: The above obtained precursors (including $\text{Co}(\text{OH})_2$ @NiCo-LDH, NiCo-LDH and ZIF-67) are further annealed in air at 300 °C for two hours to converse the precursors to mixed metal oxides.

Characterization: The X-ray diffraction patterns of the products were collected on a Rigaku-D/max 2500 V X-ray diffractometer with Cu-K α radiation ($\lambda = 1.5418 \text{ \AA}$), with an operation voltage and current maintained at 40 kV and 40 mA. Transmission electron microscopic (TEM) images were obtained with a TECNAI G2 high-resolution transmission electron microscope operating at 200 kV. XPS measurement was performed on an ESCALAB-MKII 250 photoelectron spectrometer (VG Co.) with Al K α X-ray radiation as the X-ray source for excitation.

LIBs test: The working electrode consists of 70 wt% of active material, 20 wt% of conductive carbon black, and 10 wt% of polymer binder (polyvinylidene fluoride, PVDF). The typical loading mass of the active materials is $\sim 1 \text{ mg cm}^{-2}$. The electrolyte is 1M LiPF_6 in a mixture of ethylene carbonate and diethyl carbonate (1:1 by weight). Lithium disc was used as both the counter and reference electrode. Cell assembly was carried out in an Ar-filled glovebox with moisture and oxygen concentrations below 1.0 ppm. The charge-discharge tests were performed on a LAND battery tester.

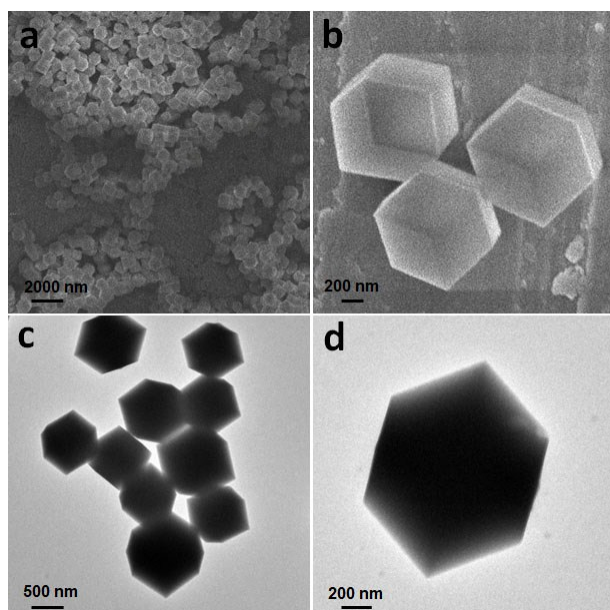


Fig. S1 SEM (a and b) and TEM images (c and d) of ZIF-67 crystals.

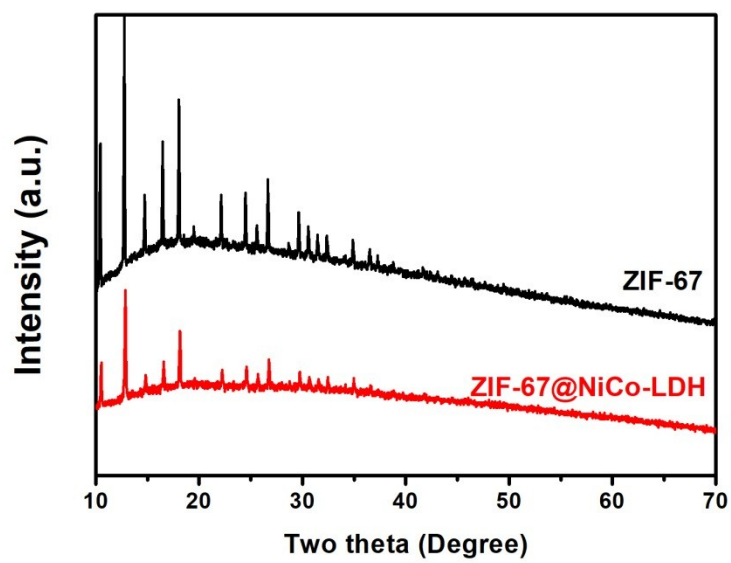


Fig. S2 XRD patterns of ZIF-67 and ZIF-67@NiCo-LDH nanoparticles.

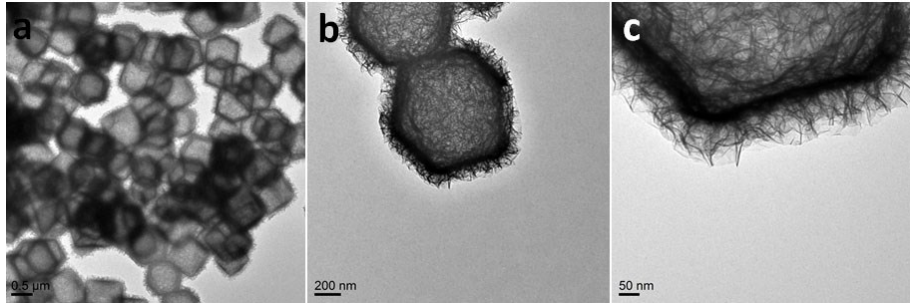


Fig. S3 TEM images of NiCo-LDH hollow cages.

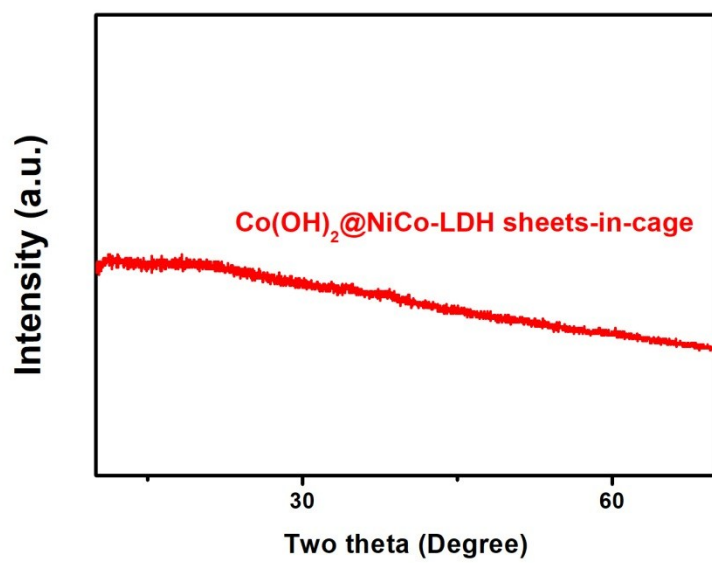


Fig. S4 XRD pattern of Co(OH)₂@NiCo-LDH nanoparticles.

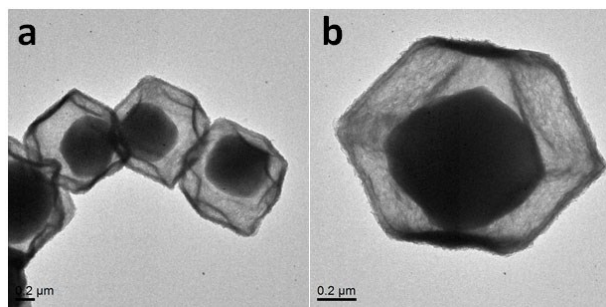


Fig. S5 TEM images of the product obtained by using pure ethanol as the solvent.

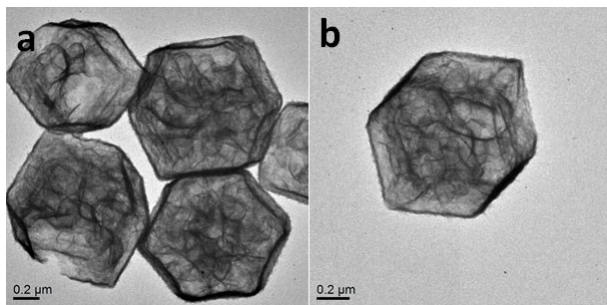


Fig. S6 TEM images of the product obtained by increasing the volume ratio of H₂O/ethanol to 2/1.

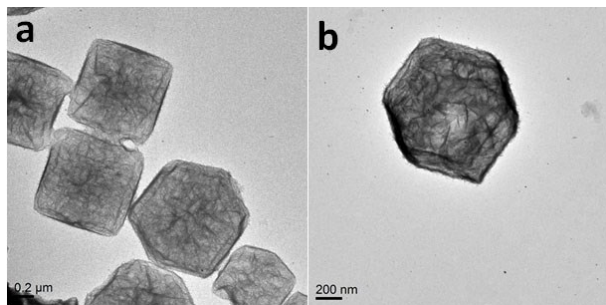


Fig. S7 TEM images of the product obtained by using urea to instead of HMT.

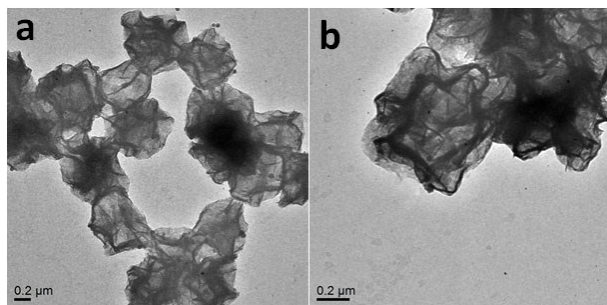


Fig. S8 TEM images of the product obtained by using ZIF-67 to react with NMT directly.

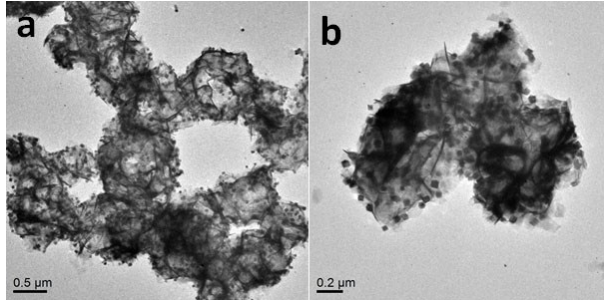


Fig. S9 TEM images of the product obtained by using $\text{NH}_3\text{H}_2\text{O}$ to replace HMT.

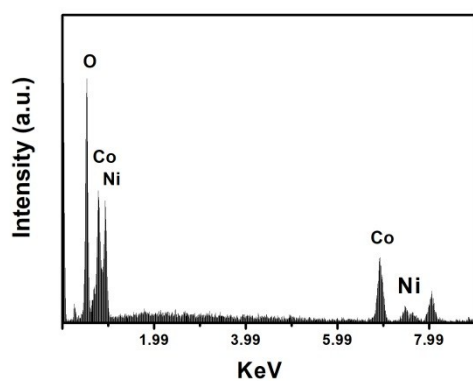


Fig. S10 EDX spectrum of $\text{Co}_3\text{O}_4@\text{NiCo}_2\text{O}_4$ sheets-in-cage nanoparticles.

For EDX analysis, the sample is previously dropped on a Cu foil. The peak at 7.99 keV could be assigned to the signal of Cu element.

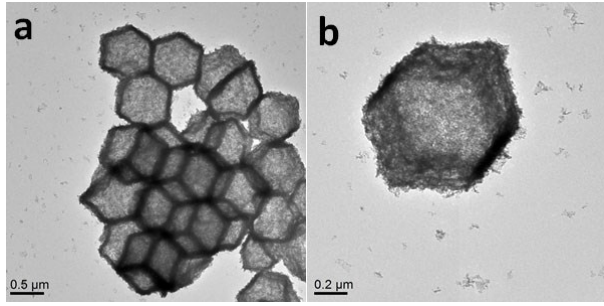


Fig. S11 TEM image of single-shelled NiCo_2O_4 nanoboxes.

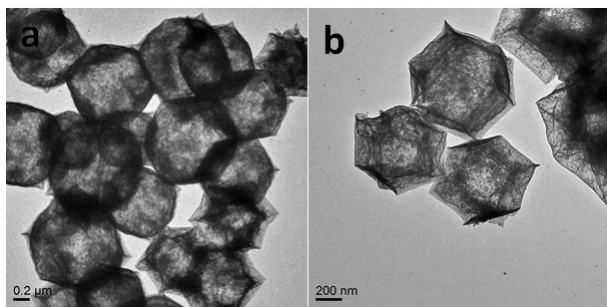


Fig. S12 TEM image of single-shelled Co_3O_4 nanoboxes.

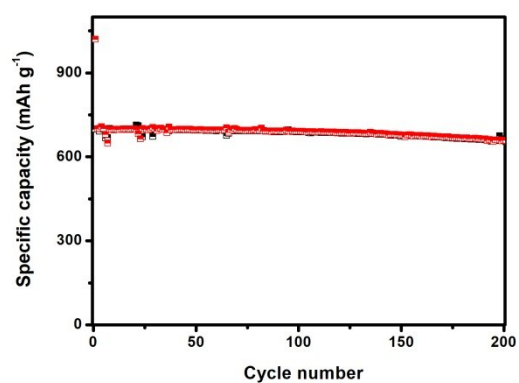


Fig. S13 Cycling performance of $\text{Co}_3\text{O}_4@\text{NiCo}_2\text{O}_4$ sheets-in-cage nanoparticles at a current density of 1 A g^{-1} .

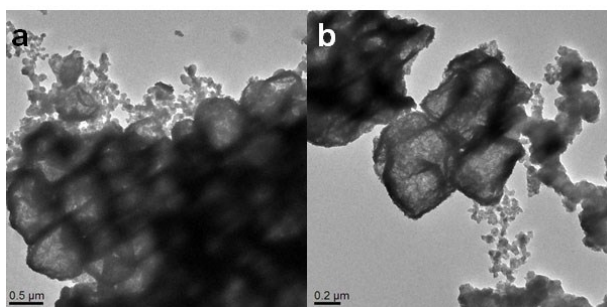


Fig. S14 TEM images of the $\text{Co}_3\text{O}_4@\text{NiCo}_2\text{O}_4$ sheets-in-cage particles after the cycling test.

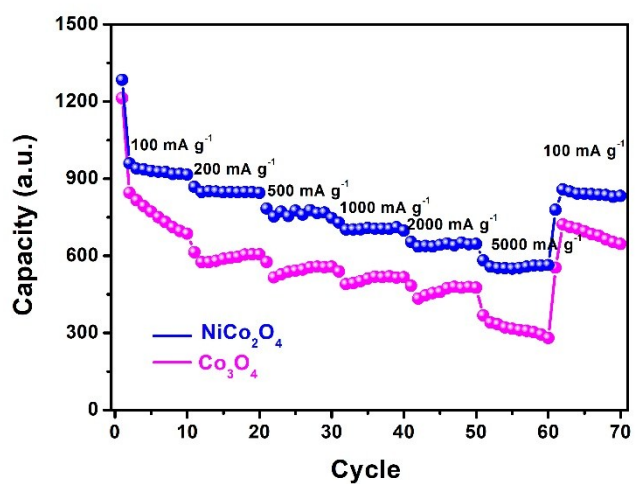


Fig. S15 Rate performance of NiCo₂O₄ and Co₃O₄ nanocages (discharge capacity).

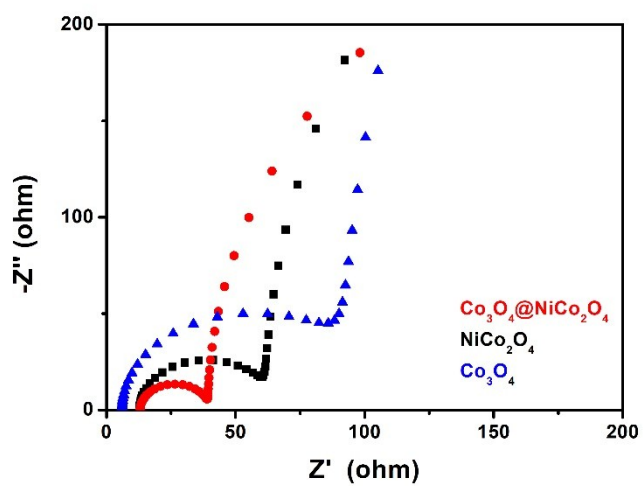


Fig. S16 Nyquist plots of the as-obtained $\text{Co}_3\text{O}_4@ \text{NiCo}_2\text{O}_4$, NiCo_2O_4 and Co_3O_4 electrodes in the frequency range from 0.1 MHz to 0.01 Hz.